

Article

Modification to L-H Kinetics Model and Its Application in the Investigation on Photodegradation of Gaseous Benzene by Nitrogen-Doped TiO₂

Peng Sun , Jun Zhang, Wenxiu Liu, Qi Wang and Wenbin Cao *

School of Materials Science and Engineering, University of Science and Technology Beijing, Beijing 100083, China; ustbsunpeng@163.com (P.S.); zhangjunustb@foxmail.com (J.Z.); liuwenxiu@outlook.com (W.L.); wangqi15@ustb.edu.cn (Q.W.)

* Correspondence: wbcao@ustb.edu.cn; Tel.: +86-010-6233-2457

Received: 11 July 2018; Accepted: 6 August 2018; Published: 9 August 2018



Abstract: In this paper, the Langmuir-Hinshelwood (L-H) model has been used to investigate the kinetics of photodegradation of gaseous benzene by nitrogen-doped TiO₂ (N-TiO₂) at 25 °C under visible light irradiation. Experimental results show that the photoreaction coefficient k_{pm} increased from $3.992 \times 10^{-6} \text{ mol}\cdot\text{kg}^{-1}\cdot\text{s}^{-1}$ to $11.55 \times 10^{-6} \text{ mol}\cdot\text{kg}^{-1}\cdot\text{s}^{-1}$ along with increasing illumination intensity. However, the adsorption equilibrium constant K_L decreased from 1139 to 597 $\text{m}^3\cdot\text{mol}^{-1}$ when the illumination intensity increased from $36.7 \times 10^4 \text{ lx}$ to $75.1 \times 10^4 \text{ lx}$, whereas it was 2761 $\text{m}^3\cdot\text{mol}^{-1}$ in the absence of light. This is contrary to the fact that K_L should be a constant if the temperature was fixed. This phenomenon can be attributed to the breaking of the adsorption-desorption equilibrium by photocatalytically decomposition. To compensate for the disequilibrium of the adsorption-desorption process, photoreaction coefficient k_{pm} was introduced to the expression of K_L and the compensation form was denoted as K_m . K_L is an indicator of the adsorption capacity of TiO₂ while K_m is only an indicator of the coverage ratio of TiO₂ surface. The modified L-H model has been experimentally verified so it is expected to be used to predict the kinetics of the photocatalytic degradation of gaseous benzene.

Keywords: modified L-H model; N-TiO₂; photocatalytic degradation; benzene

1. Introduction

Gaseous benzene released from paints, artificial panel or furniture is threatening to human health, particularly for children. However, the gaseous benzene in indoor air is difficult remedy with traditional methods due to its low concentration (ppm or ppb level) [1–3]. However, TiO₂ can decompose gaseous benzene under ultraviolet light irradiation, thus it has attracted growing attention [4–8]. In fact, the photodegradation of gaseous benzene by TiO₂ photocatalyst is a heterogeneous reaction occurring at a gas-solid interface, and the reaction rate is strongly affected by the environmental factors, particularly illumination intensity [9–11]. So the kinetic study of photocatalytic reaction is important for revealing the effect of these factors on the photocatalytic reaction rate.

The heterogeneous reaction includes two consecutive steps. Firstly, the reactants are adsorbed on the surface of the photocatalysts and secondly, the photocatalytic reaction commences. Generally, the adsorption rate is slower than the photocatalytic reaction rate. So the overall photocatalytic reaction rate is mainly dominated by the adsorption rate. Furthermore, the adsorption rate can be equivalently expressed using the coverage ratio of the adsorbed reactants on the surface of the photocatalysts [12–15]. So the photocatalytic reaction rate r can be expressed as Equation (1) [16–18], which is widely known as the original L-H model.

$$r = -\frac{dc}{dt} = k_p\theta \quad (1)$$

where c is the concentration of the reactant, t is the photocatalytic reaction time, θ is the coverage ratio of pollutants on the TiO_2 surface, k_p is photoreaction coefficient.

According to Langmuir adsorption theory, the coverage ratio is related to adsorption capacity and the concentration of the reactant. K_L was defined as adsorption equilibrium constant to measure the adsorption capacity of TiO_2 and coverage ratio θ can be expressed as Equation (2) according to adsorption theory [19].

$$\theta = \frac{K_L c}{1 + K_L c} \quad (2)$$

Input θ from Equation (2) to Equation (1), the photoreaction coefficient r can be expressed as Equation (3) [20–22],

$$r = k_p \frac{K_L c}{1 + K_L c} \quad (3)$$

Equation (3) is the much known expression of L-H model and has been widely used in investigating the kinetics of photocatalytic reactions. Lin et al. [23] studied the photocatalytic degradation pathway of dimethyl sulfide. They used original and derivative L-H models to study the kinetics under different temperatures and found that temperature can enhance photocatalytic activity. Dhada et al. [24] investigated the photocatalytic degradation of benzene by TiO_2 under sunshine and UV light. They found that UV light can promote photocatalytic reaction than visible light due to its higher energy of the photons. Cheng et al. [25] studied the photocatalytic degradation of benzene. They found that higher temperature, illumination intensity and humidity can promote the reaction rate greatly.

The works mentioned above are focused in revealing the effect of environmental factors such as illumination intensity, the amount of the photocatalyst and some processing parameters on the photodegradation ratio. However, the effect of illumination intensity on adsorption equilibrium coefficient of gaseous pollutant was neglected in most articles. In liquid phase photocatalysis, some authors have reported their research on the effect of the illumination intensity on both the photoreaction coefficient and the adsorption coefficient [26–29]. Du [30] found that the value of the adsorption coefficient calculated from the L-H model was illumination intensity-dependent in photodegradation of liquid dimethyl phthalate (DMP).

Coincidentally, it has also been found that the adsorption coefficient has been affected by light intensity in the gaseous photocatalytic reactions [31,32]. Brosillon [31] studied the kinetic model of photocatalytic degradation of butyric acid, and they found that the adsorption coefficient K_R can be expressed as Equation (4)

$$K_R = \frac{(k_{rLH} C_{Rads0} + k_{d1} + k'_{d2} I) K}{k_{d1} + k'_{d2} I} \quad (4)$$

where k_{rLH} is the reaction rate of the reaction between $\cdot\text{OH}$ and reactants, k_{d1} , k'_{d2} is the decomposition rate of $\cdot\text{OH}$ in the routes of $\cdot\text{OH} \rightarrow \text{OH}^- + \text{h}^+$ and $\cdot\text{OH} + \text{e}^- \rightarrow \text{OH}^-$, I is the light intensity, K is the adsorption constant without light irradiation. Their results indicate that the adsorption coefficient in gas photocatalytic reaction is a function of light intensity, which is not reasonable as the adsorption coefficient should be a constant under a fixed temperature. And, the parameter k_{rLH} , k_{d1} , k'_{d2} are difficult to calculate as the concentration of $\cdot\text{OH}$ is difficult to accurately measure [33] during the process of photocatalytic degradation of benzene and its concentration changes during the progression of the photocatalytic reaction. So this model is not applicable to predict the concentration of the reactant at different reaction times under different illumination intensities. He [32] investigated the degradation of benzene by mesoporous TiO_2 and also found that the adsorption coefficient could be affected by light intensity. They attributed it to the decrease of available active sites as the increased photo-induced radicals will occupy more of the active sites under higher illumination intensity. However, the effect of photocatalytic decomposition of the adsorbed benzene by the increased radicals on the adsorption coefficient was not considered. So, it's necessary to accurately describe the relationship between the adsorption coefficient and the illumination intensity in gaseous photocatalytic reactions.

In the present work, the effect of illumination intensity on photoreaction coefficient k_{pm} and adsorption equilibrium coefficient has been studied under a constant 25 °C. Photoreaction coefficient was introduced as the modification to K_L and the compensation K_m was used to replace K_L in the original L-H model. The modified L-H model can reveal the interaction between the adsorption, desorption and photo-oxidation process. The results showed that the K_m and k_{pm} can be obtained under different illumination intensity at 25 °C, thus the concentration at different reaction times can be predicted.

2. Results and Discussion

2.1. Characterization of the N-TiO₂ Photocatalysts

The N-TiO₂ catalysts were characterized by X-ray diffraction (XRD), Transmission electron microscopy (TEM), UV-Vis spectra (UV-Vis) and X-ray photoelectron spectroscopy (XPS) and the results were illustrated in Figure 1. Figure 1a shows the XRD patterns of N-TiO₂. It is clear that all the diffraction peaks were indexed to that of anatase TiO₂ (JCPDS no. 21-1272). The crystal size calculated by Scherrer's Equation was also around 10.2 nm. Figure 1b shows the morphology of the N-TiO₂ powders. It can be found that the prepared sample was composed of spherical TiO₂ and the size was ranged from 9 to 12 nm, which is in consistent with the calculated result. The light absorption spectrum was measured by UV-Vis spectrum and was shown in Figure 1c. It is well known that the bandgap of pristine anatase is 3.2 eV, while the light absorption has been extended into the ranged of 400 to 600 nm of as-prepared N-TiO₂. And its bandgap energy was 2.9 eV shown in the inset of Figure 1c calculated by using the method in other works [34,35]. The chemical state of N1s was also investigated by XPS and the result was shown in Figure 1d. Only one peak located at 399.9 eV can be found, which can be attributed to the interstitial doping of nitrogen into TiO₂ lattice with Ti–O–N bond [36].

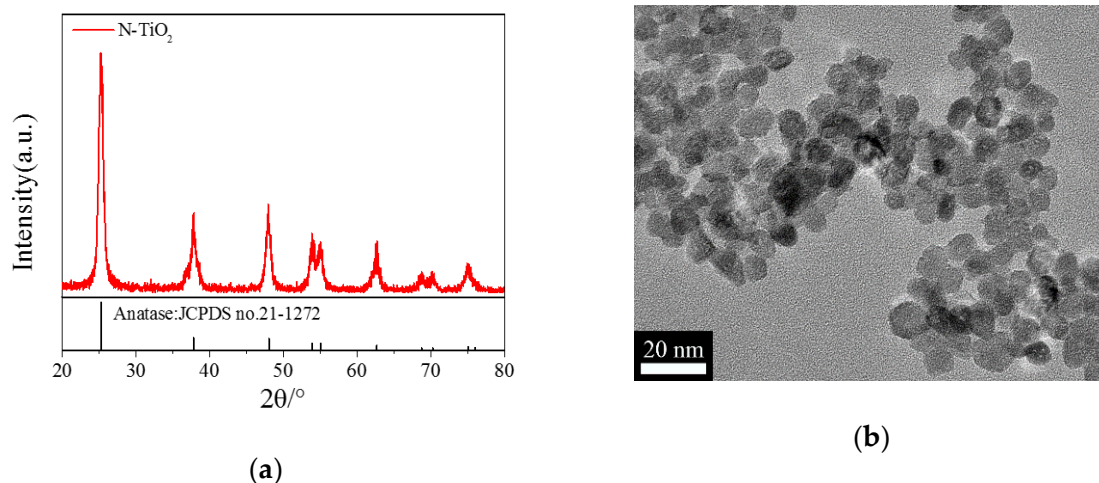


Figure 1. Cont.

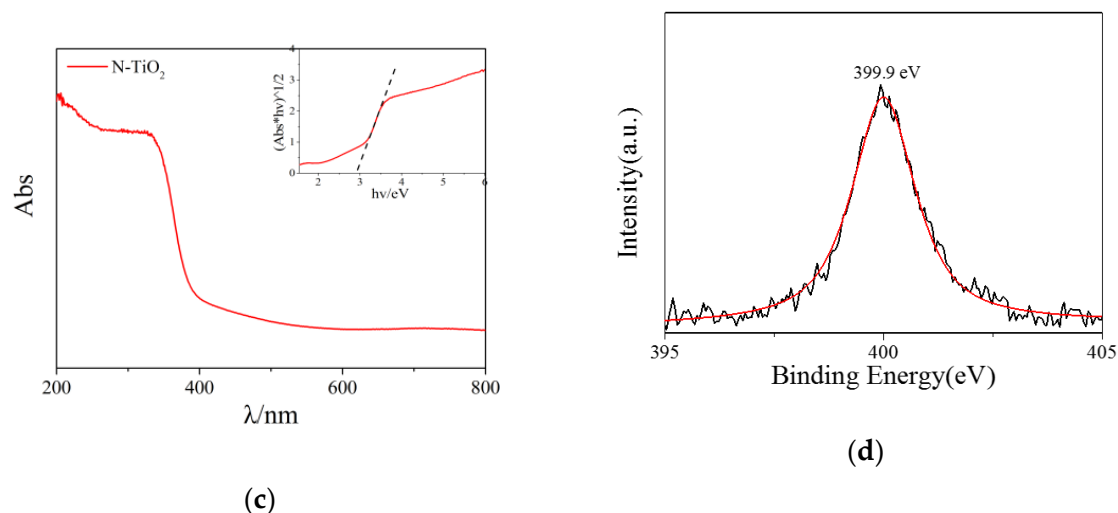


Figure 1. Characterization of N-TiO₂ catalysts (a) XRD patterns, (b) TEM image, (c) UV-Vis spectrum, (d) N1s binding energy peak.

2.2. Kinetic Study of Photocatalytic Degradation of Benzene under Different Illumination Intensity

Figure 2 shows the variation of benzene concentration with photocatalytic degradation time under different illumination intensities. It shows that the concentration of benzene remained almost unchanged during the first hour without light irradiation, indicating that adsorption and desorption processes of benzene on TiO₂ surface have reached equilibrium, thus the decrease of benzene after illumination can be ascribed to the photocatalytic degradation process. When it was illuminated for 4 h under different illumination intensity of 36.7×10^4 , 46.9×10^4 , 61.7×10^4 and 75.1×10^4 lx, the removal ratio of benzene was 72.1%, 84%, 90% and 92.4%, respectively. The removal ratio increased dramatically under higher illumination intensity, indicating that illumination intensity can promote the photocatalytic degradation performance.

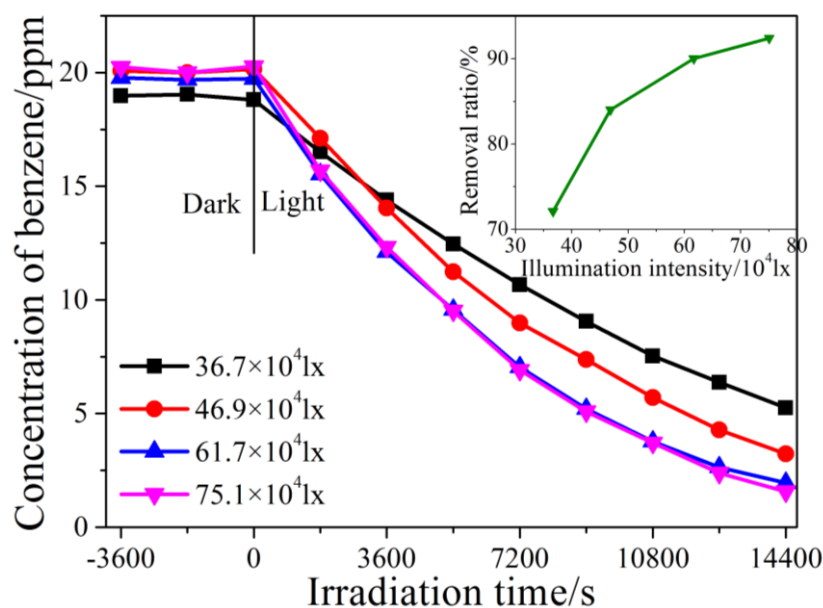


Figure 2. Variation of benzene concentration vs. photocatalytic degradation time under different illumination intensity.

During the photocatalytic degradation process, the amount of degraded benzene per unit time can be calculated by Equation (5).

$$\Delta n = rV = -\frac{dc}{dt}V \quad (5)$$

where Δn is the amount of degraded benzene per unit time, r is the photocatalytic degradation rate, V is the volume of the reactor, c is concentration of benzene and t is photocatalytic degradation time. The detailed form of r is shown by original L-H model in Equation (3) [32,37], so after inputting r from Equation (3) to Equation (5), we can get

$$\Delta n = -\frac{dc}{dt}V = k_p \frac{K_L c}{1 + K_L c} \quad (6)$$

In Equation (6), k_p is the photoreaction coefficient of the whole reaction system and is related to the mass of the catalysts. So the photocatalytic degradation rate coefficient per unit mass k_{pm} can be expressed in Equation (7)

$$k_{pm} = \frac{k_p}{m} \quad (7)$$

Input k_{pm} from Equation (7) into Equation (6), then we can get

$$-\frac{dc}{dt}V = mk_{pm} \frac{K_L c}{1 + K_L c} \quad (8)$$

So the relationship between dc and dt can be expressed in Equation (9)

$$-\frac{V}{mk_{pm}} \frac{1 + K_L c}{K_L c} dc = dt \quad (9)$$

The relationship between c and t can be obtained after making integration to Equation (9), that is

$$-\frac{V}{k_{pm}m} \int_{c_0}^c \frac{1 + K_L c}{K_L c} dc = \int_0^t dt \quad (10)$$

The result of Equation is

$$t = \frac{V}{mk_{pm}} \left[(c_0 - c) + \frac{1}{K_L} (\ln c_0 - \ln c) \right] \quad (11)$$

After rearranging in terms of $1/(c_0 - c)$, the linear form of Equation (11) is obtained.

$$\frac{\ln(c_0/c)}{c_0 - c} = \frac{m}{V} k_{pm} K_L \frac{t}{c_0 - c} - K_L \quad (12)$$

In Equation (12), it can be found that $\ln(c_0/c)/(c_0 - c)$ and $t/(c_0 - c)$ is a linear relationship, and the slope and intercept of the line is $mk_{pm}K_L/V$ and K_L respectively.

Figure 3 shows the plots of $\ln(c_0/c)/(c_0 - c)$ vs. $t/(c_0 - c)$ under different illumination intensity. According to the obtained slopes and intercepts, the values of k_{pm} and K_L were calculated and summarized in Table 1. And the standard deviation R^2 for each case were also listed in Table 1.

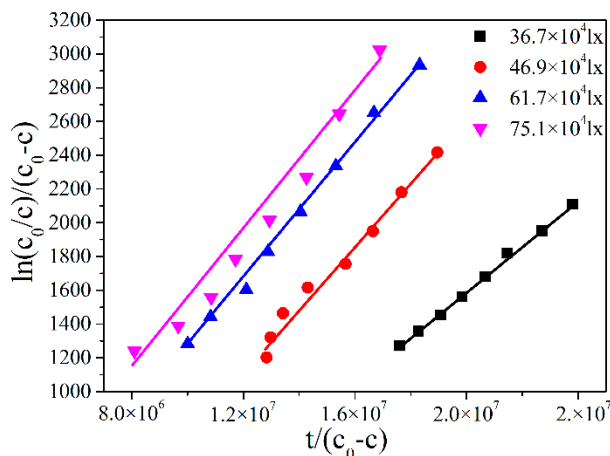


Figure 3. Plots of $\ln(c_0/c)/(c_0 - c)$ vs. $t/(c_0 - c)$ under different illumination intensity. (solid points: experimental results; solid line(curve): fitted results).

Table 1. Calculated K_{pm} and K_L under different illumination intensity using the original L-H model.

Illumination Intensity/ 10^4 lx	$k_{pm}/10^{-6} \text{ mol}\cdot\text{kg}^{-1}\cdot\text{s}^{-1}$	$K_L/\text{m}^3\cdot\text{mol}^{-1}$	R^2
36.7	3.992	1139	0.9981
46.9	5.731	1064	0.9847
61.7	8.589	791	0.9961
75.1	11.55	597	0.9674

It can be seen from Table 1 that k_{pm} was calculated as 3.992×10^{-6} , 5.371×10^{-6} , 8.589×10^{-6} , $11.55 \times 10^{-6} \text{ mol}\cdot\text{kg}^{-1}\cdot\text{s}^{-1}$ corresponding to the illumination intensity of 36.7×10^4 , 46.9×10^4 , 61.7×10^4 , and 75.1×10^4 lx, respectively. And k_{pm} increased greatly with increases in illumination intensity, which means that the photodegradation rate of benzene can be significantly promoted by increasing the illumination intensity in our experiment conditions. It's reasonable that the increased illumination intensity means more photon irradiated on TiO_2 surface, that can produce more $\cdot\text{OH}$, which is the main radical in photocatalytic reaction. According to other works [32], photoreaction rate coefficient k_{pm} depends on illumination intensity in a power law

$$k_{pm} = \alpha I^n \quad (13)$$

The value of intensity coefficient α and exponent n was 2.24×10^{-14} and 1.482 obtained by using the results in Table 1.

And the value of adsorption constant K_L was decreased from $1139 \text{ m}^3\cdot\text{mol}^{-1}$ to $597 \text{ m}^3\cdot\text{mol}^{-1}$ when the illumination intensity was increased from 36.7×10^4 lx to 75.1×10^4 lx. That is, K_L varied with the variation of the illumination intensity. However, the adsorption constant K_L is related to the temperature and should be a constant as the temperature of the reactor was carefully maintained at 25°C according to Langmuir adsorption theory. So the obtained results are inconsistent with the basic fact that the K_L should be kept unchanged if the temperature was fixed for a certain adsorption-desorption balance, which shows that original L-H model cannot be used to describe the photocatalysis processes accurately.

Generally, it is widely recognized that the photocatalytic degradation of gaseous chemicals mainly includes two steps, gas adsorption on the surface of the photocatalyst and photodegradation. After the gas chemicals were adsorbed on the surface of the photocatalyst, certain amount of the adsorbed molecules were decomposed by photocatalytic degradation.

However, the original L-H model only considers the adsorption and desorption equilibrium of the gas molecules on the surface of the photocatalyst. So the amount of the adsorbed benzene molecules Δn_a and lost desorbed benzene molecules Δn_d of N-TiO₂ surface per unit time can be defined as Equation (14) and Equation (15) respectively [38].

$$\Delta n_a = k_a c(1 - \theta)S \quad (14)$$

$$\Delta n_d = k_d \theta S \quad (15)$$

where k_a and k_d is adsorption and desorption constant of benzene and is all thermodynamic constant.

When adsorption and desorption process reach equilibrium, there is $\Delta n_a = \Delta n_d$, and the detailed form is shown in Equation (16).

$$k_a c(1 - \theta)S = k_d \theta S \quad (16)$$

So coverage ratio θ and adsorption equilibrium constant K_L can be obtained [19]

$$\theta = \frac{k_a c}{k_d + k_a c} = \frac{\frac{k_a}{k_d} c}{1 + \frac{k_a}{k_d} c} \quad (17)$$

$$K_L = \frac{k_a}{k_d} \quad (18)$$

K_L is thermodynamically constant due to k_a and k_d being thermodynamic constants, and is an indication of adsorption ability of the catalysts. While in photocatalytic reaction, the degradation process would cause the decrease of benzene on TiO₂ surface, which is equivalent to the increase in the desorption rate of benzene molecules. So the equilibrium between adsorption and desorption process would be broken. However, adsorption equilibrium constant K_L is only related to k_a and k_d in Equation (18), which make it impossible to reveal the effect of degradation process on the equilibrium. Therefore, original L-H model based on Langmuir adsorption theory is not entirely suitable for the photocatalytic degradation of benzene and necessary modification should be applied to original L-H model for better understanding kinetics of the photocatalysis process.

2.3. Modification to the L-H Model and Kinetic Results under Different Illumination Intensity

In the photocatalytic reaction, there are three processes: Adsorption, desorption and the photocatalytic degradation process. The photocatalytic degradation process will cause decrease of benzene molecules on interface, so the amount of lost benzene molecules Δn_b is the sum of desorbed and photocatalytic degraded benzene molecules per unit time.

$$\Delta n_b = k_d \theta S + k_{pm} \theta S \quad (19)$$

Combing Equation (13) and (18), the coverage ratio θ becomes

$$\theta = \frac{k_a c}{k_d + k_{pm} + k_a c} = \frac{\frac{k_a}{k_d + k_{pm}} c}{1 + \frac{k_a}{k_d + k_{pm}} c} = \frac{K_m c}{1 + K_m c} \quad (20)$$

$$K_m = \frac{k_a}{k_d + k_{pm}} = \frac{k_d}{k_d + k_{pm}} \frac{k_a}{k_d} = \frac{k_d}{k_d + k_{pm}} K_L \quad (21)$$

$k_a / (k_d + k_{pm})$ can be defined as coverage coefficient K_m in Equation (21). The coverage coefficient K_m is a function of k_a , k_d and k_{pm} , so K_m is not thermodynamic constant due to k_{pm} is photodynamic. The value of K_m is equal to that of K_L while there is no light due to k_{pm} is zero without irradiation. And the value of k_{pm} will increase greatly under high illumination intensity, thus will result in a decrease of K_m , which is in accordance with the experimental results in Table 1.

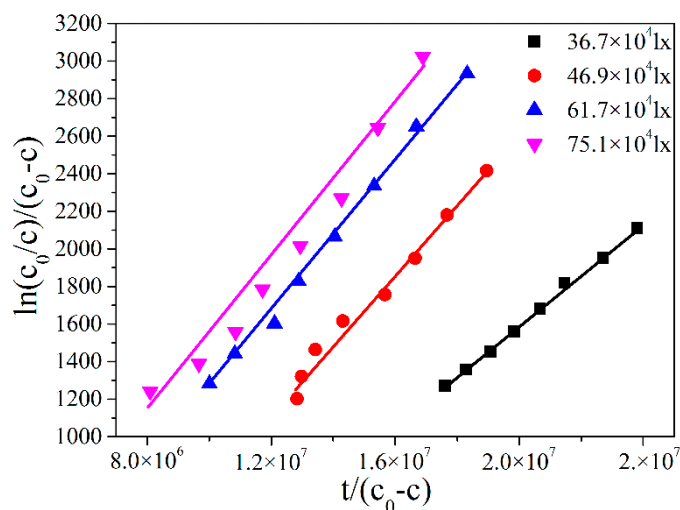
The original L-H model can be modified by using K_m to replace K_L in Equation (13) and (14) there is

$$t = \frac{V}{mk_{pm}} \left[(c_0 - c) + \frac{1}{K_m} (\ln c_0 - \ln c) \right] \quad (22)$$

$$\frac{\ln(c_0/c)}{c_0 - c} = \frac{m}{V} k_{pm} K_m t \frac{1}{c_0 - c} - K_m \quad (23)$$

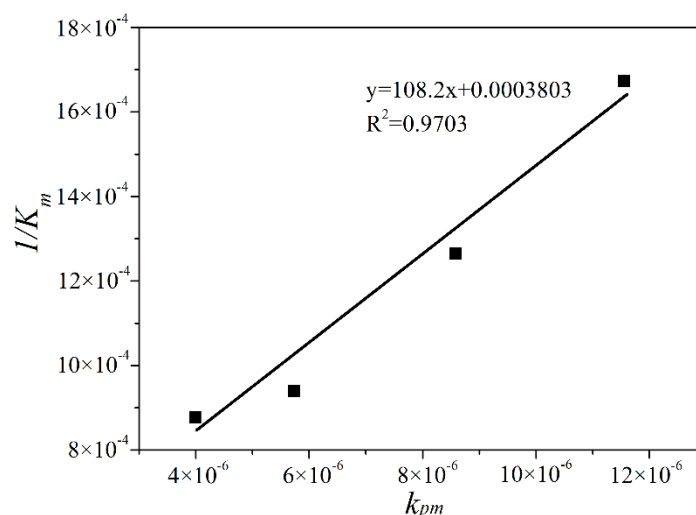
The expression form of Equation (23) is similar to that of original L-H model except coverage coefficient K_m and equilibrium coefficient K_L . K_L in original L-H model is an indicator of adsorption capacity of TiO_2 , while K_m is the indicator of the amount of benzene on TiO_2 surface. The parameters k_{pm} and K_m can be obtained through the plots of $\ln(c_0/c)/(c_0 - c)$ vs. $t/(c_0 - c)$ which were shown in Figure 4a and the results were listed in Table 2. And after taking reciprocal on both sides of Equation (21), the linear relationship exists between $1/K_m$ and k_{pm} can be found in Equation (24) and was shown in Figure 4b. Then the values of k_a , k_d and K_L can also be obtained and summarized in Table 2. The value of K_L in modified L-H model is $2629 \text{ m}^3 \cdot \text{mol}^{-1}$ under different illumination intensity at 25°C , which is consistent with Langmuir adsorption theory. The value of k_a and k_d is constant in a given temperature at 25°C and the relationship of k_{pm} and I is revealed in Equation (14), thus K_m under different illumination intensity can be obtained by Equation (21). Therefore, the concentration c at different photocatalytic reaction time t under different illumination intensity I can be predicted from Equation (22)

$$\frac{1}{K_m} = \frac{k_{pm}}{k_a} + \frac{k_d}{k_a} \quad (24)$$



(a)

Figure 4. Cont.



(b)

Figure 4. The relationship of the kinetic parameters in modified L-H model (a) The linear of $\ln(c_0/c)/(c_0 - c)$ vs. $t/(c_0 - c)$, (b) The linear of $1/K_m$ vs. k_{pm} (solid points: experimental results; solid line (curve): Fitted results).

Table 2. Results of modified L-H model under different illumination intensity.

Illumination Intensity/ 10^4 lx	Photoreaction Coefficient $k_{pm}/10^{-6} \text{ mol}\cdot\text{kg}^{-1}\cdot\text{s}^{-1}$	Coverage Coefficient $K_m/\text{m}^3\cdot\text{mol}^{-1}$	Adsorption Constant $k_a/\text{m}^3\cdot\text{kg}^{-1}\cdot\text{s}^{-1}$	Desorption Constant $k_d/\text{mol}\cdot\text{kg}^{-1}\cdot\text{s}^{-1}$	Adsorption Equilibrium Constant $K_L/\text{m}^3\cdot\text{mol}^{-1}$
36.7	3.992	1139			
46.9	5.731	1064			
61.7	8.589	791	9.242×10^{-3}	3.514×10^{-6}	2629
75.1	11.55	597			

2.4. The Adsorption Equilibrium Constant K_L Obtained by Using Adsorption Theory

In fact, the adsorption equilibrium constant K_L is thermodynamically constant and can be used to evaluate the adsorption ability. In Langmuir adsorption theory, the adsorption equilibrium constant K_L without light irradiation can be obtained as follow [39–41]:

$$\frac{c_0}{(c_T - c_0)V} = \frac{c_0}{c_m V} + \frac{1}{K_L c_m V} \quad (25)$$

where c_T is total concentration of benzene filled into the reactor, c_0 is initial concentration of gaseous benzene after adsorption equilibrium, c_m is the maximum concentration that can be adsorbed by N-TiO₂. It is obvious that there is a linear relationship between $c_0/(c_T - c_0)V$ and c_0 in Equation (25). By filling different volume of benzene into reactor, c_T and c_0 can be measured after adsorption equilibrium and were summarized in Table 3. The plot of $c_0/(c_T - c_0)V$ vs. $c_0/c_m V$ was shown in Figure 5. The slope and intercept of the linear is $1/c_m V$ and $1/K_L c_m V$, respectively. The value of K_L was $2761 \text{ m}^3\cdot\text{mol}^{-1}$, which is an indicator of the adsorption ability of benzene of N-TiO₂ at 25 °C.

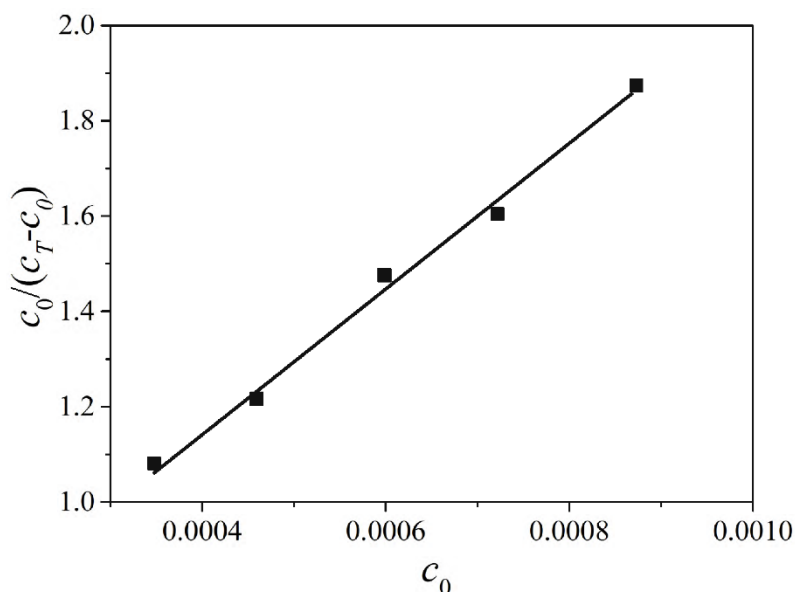


Figure 5. Linear relationship between $c_0/(c_T - c_0)$ and c_0 (solid points: experimental results; solid line(curve): fitted results).

Table 3. Concentration of benzene before and after adsorption equilibrium at 25 °C.

Total Concentration Filled into the Reactor c_t /ppm	Initial Concentration after Adsorption Equilibrium c_0 /ppm
15	7.79
18.75	10.29
22.5	13.41
26.25	16.17
30	19.56

2.5. Verification of the Modified L-H Model

To verify the modified L-H model, the photodegradation of benzene under the illumination intensity of 23.8×10^4 lx was carried out by fixing other conditions except the initial concentration of benzene was 14.81 ppm. In this case, the calculated k_{pm} and K_m is $2.101 \times 10^{-6} \text{ mol} \cdot \text{kg}^{-1} \cdot \text{s}^{-1} \text{ mol}$ and $1645 \text{ m}^3 \cdot \text{mol}^{-1}$ respectively. By inputting the values of k_{pm} and K_m into Equation (22), the predicted concentration variation of benzene vs. irradiation time was obtained, which is shown in Figure 6 (denoted with the black solid line). The experimentally measured concentration of the benzene was denoted with red solid squares in Figure 6. It is clearly seen that the theoretical prediction shows very good agreement with the experimental results. So the modified L-H model can be used to predict benzene concentration under different illumination intensities at a constant temperature.

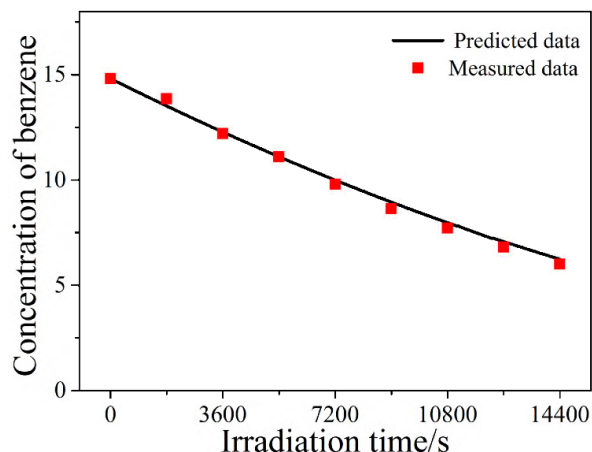


Figure 6. The predicted and measured concentration of benzene vs. time.

3. Materials and Methods

3.1. Preparation and Characterization of Samples

Nanocrystalline N-TiO₂ powders were prepared by hydrothermal method following the route used in our previous work [42]. The phase of the nano powders was determined by X-ray diffraction (XRD) with Cu K α source in the 2 θ ranging from 20 to 80°. The morphology of N-TiO₂ was characterized by Transmission electron microscopy (TEM, Hitachi, Jeol 200CX, Tokyo, Japan). UV-Vis spectra of the as-prepared sample was measured by Pgeneral UV-1901 instrument. The valence state of N was characterized by X-ray photoelectron spectroscopy (XPS, Thermo Fisher Scientific, Escalab 250, Waltham, MA, USA). Then the N-TiO₂ catalysts were dispersed into alcohol with ultrasonic wave of 50 kHz by an ultrasonicator (S6103, Aladdin, Shanghai, China) for two hours. After dispersing, the suspension was spray-coated on the surface of a SiO₂ glass substrate (5 cm \times 5 cm) and the amount of coated N-TiO₂ catalysts was 30 mg. The N-TiO₂ coated glass was dried in air under 60 °C for 2 h.

3.2. Photocatalytic Reaction System

The schematic setup of the photocatalytic reaction system is illustrated in Figure 7. The cylindrical reactor with 15 cm in height and 10 cm in diameter was made of 316 L stainless steel. The temperature of the reactor were maintained at 25 °C by a bath circulator. A xenon lamp with a cut-off filter of 420 nm was used as the visible light illumination source. The illumination intensity could be adjusted at the range of 0 to 80 $\times 10^4$ lx. A quartz window was mounted on the reactor for light irradiation. A gas chromatography (GC-2014, Shimadzu, Kyoto, Japan) was connected to the reactor to measure the concentrations of charged benzene in the reactor. The gas chromatography was equipped with Rtx-wax capillary column (Shimadzu) with 60 m in length, 0.53 mm in internal diameter and 1.0 μ m in thickness.

3.3. Photocatalytic Reaction Procedures

The N-TiO₂ loaded glass was put into the photocatalytic reaction chamber. After a leakage check, the reactor was pumped to a vacuum of 0.1 atmosphere pressure, then the reactor was irradiated for 24 h under 254 nm ultraviolet light to clean the possible pollutants that may be adsorbed on the surface of the photocatalysts and the reactor as well. After a certain volume of benzene was charged/flushed into the reactor, clean air (N₂:O₂ = 80%:20%) was flushed into the reactor until the inner pressure was balanced with the atmospheric pressure. The concentration of benzene was set at 30 ppm as much as possible. Then the reactor was kept in dark for 60 min to reach the balance of adsorption-desorption. After that, the xenon lamp was turned on to make the irradiation through the quartz window, while the illumination intensity was adjusted at 36.7 $\times 10^4$, 46.9 $\times 10^4$, 61.7 $\times 10^4$ and 75.1 $\times 10^4$ lx by

adjusting the distance between the light source and the sample. The concentration of the benzene in the reactor was measured and recorded every 30 min. The temperature of the reactor was maintained at 25 °C by a bath circulator.

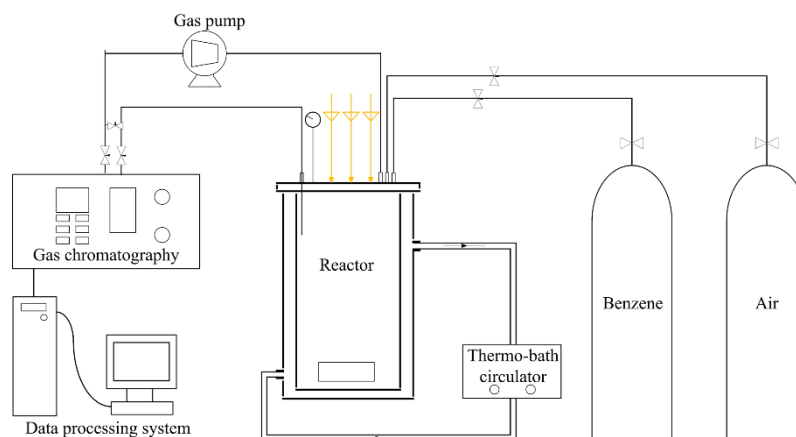


Figure 7. Schematic illustration of the photocatalytic reaction.

4. Conclusions

The L-H model has been used to investigate the kinetics of photodegradation of gaseous benzene by N-TiO₂ at 25 °C under visible light irradiation. Experimental data indicates that the adsorption equilibrium constant K_L calculated according to the L-H model decreased from 1139 to 597 m³·mol⁻¹ when the illumination intensity was increased from 36.7×10^4 lx to 75.1×10^4 lx, whereas it was 2761 m³·mol⁻¹ when in absence of light. This is contrary to the fact that K_L should be a constant if the reaction temperature was fixed. The benzene molecules adsorbed on the surface of the N-TiO₂ were dynamically photodegraded by the photocatalyst and thus the equilibrium of adsorption-desorption was broken would account for that. Photoreaction coefficient k_{pm} was introduced in the L-H model to compensate the disequilibrium of the adsorption-desorption caused by photodecomposition. Experiment result shows that k_{pm} is proportional to the light intensity $I^{1.482}$. As a result, the new parameter K_m ($k_a/(k_d + k_{pm})$) is closely related to the light intensity. Therefore, the concentration variation of benzene c vs irradiation time t under different light intensity I can be predicted.

Author Contributions: In this paper, P.S., J.Z. and W.L. designed the experiments; P.S., J.Z. and W.L. performed the experiments; P.S., J.Z., W.L. and Q.W. analyzed the data; the manuscript was written by P.S. and edited by W.C.

Funding: This research was funded by the National Key Research and Development Plan of China [Grant Nos. 2016YFC0700901, 2016YFC0700607].

Acknowledgments: This work is financially supported by the National Key Research and Development Plan of China [Grant Nos. 2016YFC0700901, 2016YFC0700607].

Conflicts of Interest: The authors declare no conflict of interest.

References

1. Sui, H.; Zhang, T.; Cui, J.; Li, X.; Crittenden, J.; Li, X.; He, L. Novel off-gas treatment technology to remove volatile organic compounds with high concentration. *Ind. Eng. Chem. Res.* **2016**, *55*, 2594–2603. [[CrossRef](#)]
2. Jiang, N.; Hui, C.-X.; Li, J.; Lu, N.; Shang, K.-F.; Wu, Y.; Mizuno, A. Improved performance of parallel surface/packed-bed discharge reactor for indoor VOCs decomposition: Optimization of the reactor structure. *J. Phys. D Appl. Phys.* **2015**, *48*, 40. [[CrossRef](#)]
3. Ye, C.Z.; Ariya, P.A. Co-adsorption of gaseous benzene, toluene, ethylbenzene, m-xylene (btex) and SO₂ on recyclable Fe₃O₄ nanoparticles at 0–101% relative humidities. *J. Environ. Sci.* **2015**, *31*, 164–174. [[CrossRef](#)] [[PubMed](#)]

4. Zeng, L.; Lu, Z.; Li, M.; Yang, J.; Song, W.; Zeng, D.; Xie, C. A modular calcination method to prepare modified N-doped TiO₂ nanoparticle with high photocatalytic activity. *Appl. Catal. B Environ.* **2016**, *183*, 308–316. [[CrossRef](#)]
5. Ren, L.; Mao, M.; Li, Y.; Lan, L.; Zhang, Z.; Zhao, X. Novel photothermocatalytic synergetic effect leads to high catalytic activity and excellent durability of anatase TiO₂ nanosheets with dominant {001} facets for benzene abatement. *Appl. Catal. B Environ.* **2016**, *198*, 303–310. [[CrossRef](#)]
6. Yadav, H.M.; Kim, J.-S. Solvothermal synthesis of anatase TiO₂-graphene oxide nanocomposites and their photocatalytic performance. *J. Alloys Compd.* **2016**, *688*, 123–129. [[CrossRef](#)]
7. Fujimoto, T.M.; Ponczek, M.; Rochetto, U.L.; Landers, R.; Tomaz, E. Photocatalytic oxidation of selected gas-phase VOCs using UV light, TiO₂, and TiO₂/Pd. *Environ. Sci. Pollut. Res.* **2017**, *24*, 6390–6396. [[CrossRef](#)] [[PubMed](#)]
8. Wongaree, M.; Chiarakorn, S.; Chuangchote, S.; Sagawa, T. Photocatalytic performance of electrospun CNT/TiO₂ nanofibers in a simulated air purifier under visible light irradiation. *Environ. Sci. Pollut. Res.* **2016**, *23*, 21395–21406. [[CrossRef](#)] [[PubMed](#)]
9. Sabbaghi, S.; Mohammadi, M.; Ebadi, H. Photocatalytic degradation of benzene wastewater using PANI-TiO₂ nanocomposite under UV and solar light radiation. *J. Environ. Eng.* **2016**, *142*, 05015003. [[CrossRef](#)]
10. Fang, J.; Chen, Z.; Zheng, Q.; Li, D. Photocatalytic decomposition of benzene enhanced by the heating effect of light: Improving solar energy utilization with photothermocatalytic synergy. *Catal. Sci. Technol.* **2017**, *7*, 3303–3311. [[CrossRef](#)]
11. Lan, L.; Li, Y.; Zeng, M.; Mao, M.; Ren, L.; Yang, Y.; Liu, H.; Yun, L.; Zhao, X. Efficient UV-Vis-Infrared light-driven catalytic abatement of benzene on amorphous manganese oxide supported on anatase TiO₂ nanosheet with dominant {001} facets promoted by a photothermocatalytic synergetic effect. *Appl. Catal. B Environ.* **2017**, *203*, 494–504. [[CrossRef](#)]
12. Melián, E.P.; Díaz, O.G.; Araña, J.; Rodríguez, J.M.D.; Rendón, E.T.; Melián, J.A.H. Kinetics and adsorption comparative study on the photocatalytic degradation of o-, m- and p-cresol. *Catal. Today* **2007**, *129*, 256–262. [[CrossRef](#)]
13. Chen, M.; Bao, C.; Cun, T.; Huang, Q. One-pot synthesis of ZnO/oligoaniline nanocomposites with improved removal of organic dyes in water: Effect of adsorption on photocatalytic degradation. *Mater. Res. Bull.* **2017**, *95*, 459–467. [[CrossRef](#)]
14. Zhi, Y.; Li, Y.; Zhang, Q.; Wang, H. ZnO nanoparticles immobilized on flaky layered double hydroxides as photocatalysts with enhanced adsorptivity for removal of acid red g. *Langmuir* **2010**, *26*, 15546–15553. [[CrossRef](#)] [[PubMed](#)]
15. Dong, W.; Lee, C.W.; Lu, X.; Sun, Y.; Hua, W.; Zhuang, G.; Zhang, S.; Chen, J.; Hou, H.; Zhao, D. Synchronous role of coupled adsorption and photocatalytic oxidation on ordered mesoporous anatase TiO₂-SiO₂ nanocomposites generating excellent degradation activity of rhb dye. *Appl. Catal. B Environ.* **2010**, *95*, 197–207. [[CrossRef](#)]
16. Kim, S.B.; Hong, S.C. Kinetic study for photocatalytic degradation of volatile organic compounds in air using thin film TiO₂ photocatalyst. *Appl. Catal. B Environ.* **2002**, *35*, 305–315. [[CrossRef](#)]
17. Golshan, M.; Zare, M.; Goudarzi, G.; Abtahi, M.; Babaei, A.A. Fe₃O₄@hap-enhanced photocatalytic degradation of Acid Red73 in aqueous suspension: Optimization, kinetic, and mechanism studies. *Mater. Res. Bull.* **2017**, *91*, 59–67. [[CrossRef](#)]
18. Deng, X.-Q.; Liu, J.-L.; Li, X.-S.; Zhu, B.; Zhu, X.; Zhu, A.-M. Kinetic study on visible-light photocatalytic removal of formaldehyde from air over plasmonic Au/TiO₂. *Catal. Today* **2017**, *281*, 630–635. [[CrossRef](#)]
19. Langmuir, I. The constitution and fundamental properties of solids and liquids. Part I. Solids. *J. Am. Chem. Soc.* **1916**, *38*, 2221–2295. [[CrossRef](#)]
20. Liu, P.; Yu, X.; Wang, F.; Zhang, W.; Yang, L.; Liu, Y. Degradation of formaldehyde and benzene by TiO₂ photocatalytic cement based materials. *J. Wuhan Univ. Technol.-Mater. Sci. Ed.* **2017**, *32*, 391–396. [[CrossRef](#)]
21. Yuzawa, H.; Aoki, M.; Otake, K.; Hattori, T.; Itoh, H.; Yoshida, H. Reaction mechanism of aromatic ring hydroxylation by water over platinum-loaded titanium oxide photocatalyst. *J. Phys. Chem. C* **2012**, *116*, 25376–25387. [[CrossRef](#)]
22. Einaga, H.; Mochiduki, K.; Teraoka, Y. Photocatalytic oxidation processes for toluene oxidation over TiO₂ catalysts. *Catalysts* **2013**, *3*, 219. [[CrossRef](#)]

23. Lin, Y.-H.; Hsueh, H.-T.; Chang, C.-W.; Chu, H. The visible light-driven photodegradation of dimethyl sulfide on S-doped TiO₂: Characterization, kinetics, and reaction pathways. *Appl. Catal. B Environ.* **2016**, *199*, 1–10. [[CrossRef](#)]
24. Dhada, I.; Nagar, P.K.; Sharma, M. Photo-catalytic oxidation of individual and mixture of benzene, toluene and p-xylene. *Int. J. Environ. Sci. Technol.* **2016**, *13*, 39–46. [[CrossRef](#)]
25. Cheng, L.; Kang, Y.; Li, G. Effect factors of benzene adsorption and degradation by nano-TiO₂ immobilized on diatomite. *J. Nanomaterials* **2012**, *2012*, 6. [[CrossRef](#)]
26. Ollis, D.F. Kinetics of liquid phase photocatalyzed reactions: An illuminating approach. *J. Phys. Chem. B* **2005**, *109*, 2439–2444. [[CrossRef](#)] [[PubMed](#)]
27. Xu, Y.; Langford, C.H. Variation of langmuir adsorption constant determined for TiO₂-photocatalyzed degradation of acetophenone under different light intensity. *J. Photochem. Photobiol. A Chem.* **2000**, *133*, 67–71. [[CrossRef](#)]
28. Giovannetti, R.; Rommozzi, E.; D'Amato, C.; Zannotti, M. Kinetic model for simultaneous adsorption/photodegradation process of alizarin red s in water solution by nano-TiO₂ under visible light. *Catalysts* **2016**, *6*, 84. [[CrossRef](#)]
29. Silva, C.G.; Faria, J.L. Effect of key operational parameters on the photocatalytic oxidation of phenol by nanocrystalline sol-gel TiO₂ under uv irradiation. *J. Mol. Catal. A Chem.* **2009**, *305*, 147–154. [[CrossRef](#)]
30. Du, E.; Zhang, Y.X.; Zheng, L. Photocatalytic degradation of dimethyl phthalate in aqueous TiO₂ suspension: A modified langmuir–hinshelwood model. *React. Kinet. Catal. Lett.* **2009**, *97*, 83–90. [[CrossRef](#)]
31. Brosillon, S.; Lhomme, L.; Vallet, C.; Bouzaza, A.; Wolbert, D. Gas phase photocatalysis and liquid phase photocatalysis: Interdependence and influence of substrate concentration and photon flow on degradation reaction kinetics. *Appl. Catal. B Environ.* **2008**, *78*, 232–241. [[CrossRef](#)]
32. He, F.; Li, J.; Li, T.; Li, G. Solvothermal synthesis of mesoporous TiO₂: The effect of morphology, size and calcination progress on photocatalytic activity in the degradation of gaseous benzene. *Chem. Eng. J.* **2014**, *237*, 312–321. [[CrossRef](#)]
33. Soltani, T.; Lee, B.-K. Novel and facile synthesis of Ba-doped BiFeO₃ nanoparticles and enhancement of their magnetic and photocatalytic activities for complete degradation of benzene in aqueous solution. *J. Hazard. Mater.* **2016**, *316*, 122–133. [[CrossRef](#)] [[PubMed](#)]
34. Chen, S.-H.; Hsiao, Y.-C.; Chiu, Y.-J.; Tseng, Y.-H. A simple route in fabricating carbon-modified titania films with glucose and their visible-light-responsive photocatalytic activity. *Catalysts* **2018**, *8*, 178. [[CrossRef](#)]
35. Li, C.X.; Jin, H.Z.; Yang, Z.Z.; Yang, X.; Dong, Q.Z.; Li, T.T. Preparation and photocatalytic properties of mesoporous RGO/TiO₂ composites. *J. Inorg. Mater.* **2017**, *32*, 357–364.
36. Xu, J.; Liu, Q.; Lin, S.; Cao, W. One-step synthesis of nanocrystalline N-doped TiO₂ powders and their photocatalytic activity under visible light irradiation. *Res. Chem. Intermed.* **2013**, *39*, 1655–1664. [[CrossRef](#)]
37. Wang, J.; Ruan, H.; Li, W.; Li, D.; Hu, Y.; Chen, J.; Shao, Y.; Zheng, Y. Highly efficient oxidation of gaseous benzene on novel Ag₃VO₄/TiO₂ nanocomposite photocatalysts under visible and simulated solar light irradiation. *J. Phys. Chem. C* **2012**, *116*, 13935–13943. [[CrossRef](#)]
38. Cong, Y.; Zhang, J.; Chen, F.; Anpo, M.; He, D. Preparation, photocatalytic activity, and mechanism of nano-TiO₂ co-doped with nitrogen and iron (iii). *J. Phys. Chem. C* **2007**, *111*, 10618–10623. [[CrossRef](#)]
39. Foo, K.Y.; Hameed, B.H. Insights into the modeling of adsorption isotherm systems. *Chem. Eng. J.* **2010**, *156*, 2–10. [[CrossRef](#)]
40. Wei, D.; Li, S.; Fang, L.; Zhang, Y. Effect of environmental factors on enhanced adsorption and photocatalytic regeneration of molecular imprinted TiO₂ polymers for fluoroquinolones. *Environ. Sci. Pollut. Res.* **2018**, *25*, 6729–6738. [[CrossRef](#)] [[PubMed](#)]
41. Li, Z.; Kim, J.K.; Chaudhari, V.; Mayadevi, S.; Campos, L.C. Degradation of metaldehyde in water by nanoparticle catalysts and powdered activated carbon. *Environ. Sci. Pollut. Res.* **2017**, *24*, 17861–17873. [[CrossRef](#)] [[PubMed](#)]
42. Xu, J.; Sun, P.; Zhang, X.; Jiang, P.; Cao, W.; Chen, P.; Jin, H. Synthesis of N-doped TiO₂ with different nitrogen concentrations by mild hydrothermal method. *Mater. Manuf. Processes* **2014**, *29*, 1162–1167. [[CrossRef](#)]

